Applied Clay Science 51 (2011) 202–208

Contents lists available at ScienceDirect

Applied Clay Science

journal homepage: www.elsevier.com/locate/clay

Note

In-situ FTIR analyses of bentonite under high-pressure

Frederico Gil Alabarse [a,*], Rommulo Vieira Conceição [a,b,1], Naira Maria Balzaretti [a,c,1], Flávia Schenato [d], Ana Maria Xavier [e]

[a] Programa de Pós-Graduação em Ciências dos Materiais, Universidade Federal do Rio Grande do Sul, PGCIMAT/UFRGS, Av. Bento Gonçalves, 9500, CEP 91501-970, P.O.BOX 15051, Porto Alegre, RS, Brazil
[b] Instituto de Geologia, Universidade Federal do Rio Grande do Sul, IG/UFRGS, Av. Bento Gonçalves, 9500-Prédio 43126, Sala 206B, Bairro Agronomia, Caixa Postal: 15.001 CEP: 91501970, Porto Alegre, RS, Brazil
[c] Instituto de Física, Universidade Federal do Rio Grande do Sul, IF/UFRGS, Av. Bento Gonçalves, 9500, Campus do Vale, CEP 91501-970, Porto Alegre, RS, Brazil
[d] Programa de Pós-Graduação em Engenharia: Energia, Ambiente e Materiais, Universidade Luterana do Brasil, PPGEAM/ULBRA, Av. Farroupilha 8001, CEP: 92425-900, Canoas, RS, Brazil
[e] Escritório de Porto Alegre da, Comissão Nacional de Energia Nuclear, ESPOA/CNEN, Av. Bento Gonçalves, 9500, CEP 91501-970, P.O. Box 15016, Porto Alegre, RS, Brazil

ARTICLE INFO

Article history:
Received 29 March 2010
Received in revised form 12 November 2010
Accepted 12 November 2010
Available online 23 November 2010

Keywords:
FTIR
Diamond anvil cell
High pressure
Montmorillonite
Bentonite

ABSTRACT

The stability of bentonite is of particular interest for containment barriers in nuclear waste disposal facilities. However, very little is known about the stability of montmorillonite (the major component of bentonite) under high-pressure (HP) conditions. The objective of this work is to investigate the stability of montmorillonite under HP conditions, using a sample of bentonite in which the major component is a dioctahedral calcium montmorillonite. This montmorillonite was characterized by Fourier transform infrared spectroscopy (FTIR), X-ray diffraction (XRD), X-ray fluorescence (XRF), specific surface area (SA), thermogravimetric analysis (TGA) and differential thermal analysis (DTA). HP experiments up to 7.7 GPa at room temperature (RT) were performed using toroidal chambers (TC). The samples were characterized by XRD after the HP processing. In-situ FTIR analyses were performed in the samples inside a diamond anvil cell (DAC) up to 8 GPa (dispersed in KBr) and up to 13 GPa (pure bentonite). In-situ FTIR measurements inside the DAC showed that montmorillonite was stable despite a reversible deformation in the Si–O bond and did not lose water up to 13 GPa. XRD analysis of the samples processed at 8 GPa at RT inside the TC showed no marked modification in the (001) reflections and b-parameter (060) reflections of montmorillonite induced by high pressure. The obtained results indicated that montmorillonite remained stable under high pressure conditions.

1. Introduction

The disposal of high-level radioactive waste in a facility located underground in a stable geological formation is currently considered a safe solution to ensure the long-term isolation from the biosphere of the radionuclides present in the radioactive waste. The construction of geological disposal facilities can be conducted in preexisting mines or in sites specially mined and engineered for such purpose. The excavation work creates a potential and preferential pathway for water, gas and radionuclides migration, and the facility has to be effectively sealed afterwards (IAEA, 2006). Backfilling and sealing of shafts, galleries and all access routes, as well as the demonstration of the feasibility of the sealing on a representative time scale are essential parts of underground repository designs.

For more than 10 years, the applicability of highly compacted bentonite has been investigated for sealing purposes. Several different types of clay minerals have been used to minimize the diffusion of contaminants from waste disposal sites, especially due to their high swelling property, sealing ability, long-term structural stability and large ion exchange capacity in the nanometric scale interlamellar space (Madejová et al., 2002; Van Geet et al., 2007).

Bentonite, a rock mostly composed by montmorillonite, is considered an important component in nuclear waste disposal facilities as part of the multi-barrier system in order to provide high degree of containment and the necessary degree of isolation from the biosphere (IAEA, 2006; Pusch, 2006). Hydration and swelling, dispersion, adsorption and ion exchange properties of the clay mineral are important factors affecting the bentonite ability to act as a clay barrier (Madejová et al., 2002). The high pressure effect on the smectite structure, morphology, hydration conditions and surface is one aspect to be investigated since there are very few studies reported in the literature that focus on this subject. Bentonites in underground nuclear repositories may be submitted to high pressure conditions and to geological events, such as seismic, tectonic and,

* Corresponding author. Tel.: +55 51 3308 6489; fax: +55 51 3308 7286.
E-mail addresses: frederico@lpmc.univ-montp2.fr (F.G. Alabarse), rommulo.conceicao@ufrgs.br (R.V. Conceição), naira@if.ufrgs.br (N.M. Balzaretti), flavia.schenato@ulbra.br (F. Schenato), axavier@cnen.gov.br (A.M. Xavier).
[1] Tel.: +55 51 3308 6489; fax: +55 51 3308 7286.

0169-1317
doi:10.1016/j.clay.2010.11.017

eventually, metamorphism. Nakazawa et al. (1992), for instance, is one of the few references reporting high pressure and high temperature synthesis of smectite.

The aim of this study was to investigate the stability of montmorillonite at very high pressures at room temperature using a toroidal-type chamber (TC) and diamond anvil cell (DAC). In-situ FTIR measurements under high pressure conditions were performed with the DAC experiments.

2. Experimental methods

2.1. Starting material

The bentonite sample was collected at Aceguá region (south of Brazil), close to the border of Brazil and Uruguay.

Bulk bentonite was first gently ground and separated intro fractions with grains smaller that <2 μm by centrifugation and sedimentation. Samples of bentonite were air dried at room temperature and later compacted for experiments in the toroidal chamber.

2.2. High pressure processing

2.2.1. Toroidal chamber experiments

High pressure experiments were performed in a high-pressure toroidal-type chamber. A detailed description of this high-pressure apparatus is given elsewhere (Alabarse, 2009; Khvostantsev, 1984; Sherman and Stadtmuller, 1987). The pressure cells consisted of a graphite heater (height of 9.2 mm, diameter of 7.0 mm, and wall thickness of 1.5 mm), and two small disks of pyrophyllite calcinated at 1000 °C (diameter of 4.0 mm and height of 1.5 mm). All experiments were conducted inside a hexagonal boron nitride (hBN) capsule (3.0 mm internal diameter), which acts as a nearly isostatic pressure-transmitting medium. This capsule containing the sample was placed in-between the pyrophyllite disks. In a typical experiment, pressure was initially applied to the sample cell to a particular value at room temperature (RT) and kept for 30 min, for pressure stabilization. The pressure calibration was performed by the "fixed points" technique, using Bi and Yb: Bi with phase transitions at 2.5 and 7.7 GPa, and Yb with a phase transition at 4.0 GPa (Sherman and Stadtmuller, 1987). The pressure was considered accurate to ±0.5 GPa (Alabarse, 2009). After the run, the samples were ground in an agate mortar just before XRD and FTIR analysis.

2.2.2. Diamond anvil cell experiments

A Piermarini-Block diamond anvil cell (DAC) (Piermarini and Block, 1975) was used. The bentonite powder was placed in a 250 μm diameter hole drilled in a Waspaloy gasket preindented to a thickness of 80 μm, along with a small ruby as pressure gauge (Piermarini et al., 1975). A mixture of 1% m/m of bentonite in KBr and pure bentonite was investigated separately by in-situ FTIR spectroscopy, respectively up to 8 and 13 GPa.

2.3. Analytical techniques

In-situ infrared transmission spectroscopy was performed on samples under pressure in the DAC experiments and measured in a Bomem FTIR model MB100, equipped with a DTGS detector and KBr beam splitter, in the spectral range from 350 to 4000 cm^{-1}, 512 scans at 4 cm^{-1} resolution. Pressure was determined with the ruby technique (Piermarini et al., 1975) with an accuracy of ±0.2 GPa (Alabarse, 2009).

X-ray diffraction (XRD) analysis was performed on random and oriented powders. Air-dried (AD), ethylene glycol-solvated (EG), and heated (calcinated, 550 °C, 2 h) samples were investigated. The mineral phases of the bulk samples were examined using a Siemens D-500 powder diffractometer equipped with Soller slits in the incident beam, 1° divergence slit, 0.15 mm entrance slit, and a graphite monochromator in the secondary beam. Data were collected with CuK_{α} radiation, in the angular range from 2° to 80° (2θ), with a step size of 0.05° and counting time of 2 s per step for all samples. The (060) reflection for determining the b parameter was registered between 58° and 64° (2θ) with a step scan of 0.02° and counting time of 8 s per step.

Chemical analyses of the bulk samples were performed by X-ray fluorescence (XRF) on a RIGAKU equipment, model RIX 2000. The sample was melted in a platinum crucible during 3 min at 1200 °C resulting in a vitrified pallet for XRF analysis. The loss on ignition was measured by thermogravimetry.

The specific surface area was determined by the BET multipoint method (Brunauer et al., 1938) on the basis of nitrogen adsorption isotherms of the samples previously degassed at 150 °C. The isotherms were determined at the liquid nitrogen boiling point in a homemade volumetric apparatus, with a vacuum line system employing a turbo molecular Edwards vacuum pump, and the pressure was measured with a capillary Hg manometer.

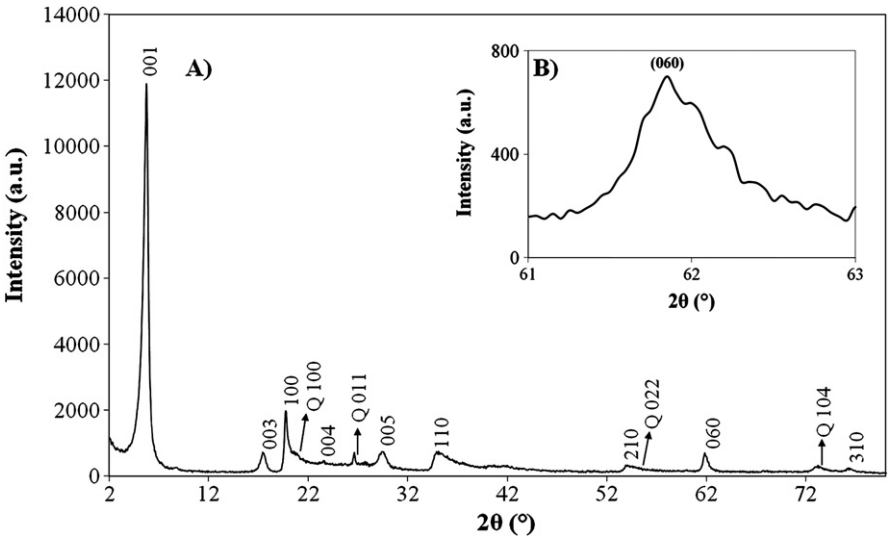

Fig. 1. A) X-ray diffraction pattern of bulk bentonite (air dried—random powder AD) and Miller indexes (Table 1). B) (060) reflection at 1.50 Å.

Table 1
Miller indexes and values of the montmorillonite (B1) and the typical XRD patterns of montmorillonite (Rosenquist, 1959).

Miller index	(001)	(003)	(100)	(004)	(005)	(110)	(210)	(060)	(310)
D(Å)	15.00	5.01	4.50	3.77	3.02	2.58	1.70	1.50	1.24
D(Å)–B1	15.36	5.08	4.49	3.77	3.02	2.57	1.70	1.50	1.24

Thermogravimetric analyses (TGA) were carried out on a Shimadzu system model TGA-50 from room temperature (RT) to 800 °C for the TGA/TDA analyses and to 1000 °C for measuring the loss of ignition, using a heating rate of 20 °C/min in argon atmosphere.

3. Results and discussions

3.1. Bentonite

3.1.1. X-ray diffraction analysis

XRD pattern of the bulk bentonite showed mainly smectite characterized by the 001 reflection and minor impurities of quartz (Fig. 1A). XRD analyses of air-dried samples (powder diffraction) presented the characteristic reflections corresponding to d values of 15.4 Å (001), 5.1 Å (003), 3.8 Å (004) and 3.0 Å (005), which were in agreement with the basal values for smectites (Table 1) (Bergaya et al., 2006; Greene-Kelly, 1953; Rosenquist, 1959). The b-parameter (from the 060 reflection) at 1.50 Å (Fig. 1B) corresponds to a dioctahedral smectite in which the high intensity of d_{060} reflection indicated a large size of the coherent domains along the b direction (Calarge 2001; Calarge et al., 2003).

Fig. 2 shows the basal reflections in air-dried (AD), ethylene glycol solvated (EG), calcinated (550 °C, 2 h) state of oriented samples. The d values of the basal reflections of the EG solvated sample were 16.6 Å (001), 8.3 Å and 5.6 Å (Fig. 3) and changed to 9.5 Å (001) during the collapse of the structure induced by heating.

The d_{001} value around 15 Å (air-dried sample) corresponds to calcium montmorillonite (Bergaya et al., 2006; Rosenquist, 1959).

The XRD data related to calcium montmorillonite were in agreement with the chemical analysis. The profiles of the basal reflections of the smectite in XRD patterns (Figs. 1–3) indicated a relatively well ordered montmorillonite.

3.1.2. Chemical composition

The bulk bentonite chemical composition (Table 2) determined by XRF, showed high contents of silicon and CaO.

The structural formula calculated for the smectite (Eq. (1)) content of bulk bentonite was determined by Calarge et al. (2003), by XRF, and was in agreement with the calcium montmorillonite compositions as the predominant phase in the bentonite sample. The montmorillonite content in bentonite determined by Calarge et al. (2003) was calculated by XRD analyses of Greene-Kelly (1953) and presents minor impurities of quartz. Calcium was the main interlayer cation of montmorillonite and the sum of the exchangeable ions (Ca^{2+}, K^{+}) of 0.47 per half formula unit indicated a high-charge smectite.

$$[Si_{3.87}Al_{0.13}]O_{10}\left(Al_{1.43}Fe^{3+}_{0.08}Mg_{0.53}Ti_{0.01}\right)(OH)_2\ K^{+}_{0.01}Ca^{2+}_{0.2} \quad (1)$$

The specific surface area of the bulk bentonite measured by BET was 67 m^2/g.

3.1.3. Infrared spectra

The FTIR spectrum in Fig. 4 of the bentonite fraction was measured in transmittance (mixture of 3 mg samples with 300 mg KBr). According to Farmer (1974), the 3621 cm^{-1} and 916 cm^{-1} bands are typical of dioctahedral smectites (Borchardt, 1977; Caillére et al., 1982). The bands at 3670 cm^{-1} and 848 cm^{-1} (Al–OH–Mg bonds) and the weak 788 cm^{-1} band (Fe^{3+}–OH–Mg bonds) indicated that the smectite was Mg-rich and Fe^{3+} depleted. The bands at 628 cm^{-1} and 670 cm^{-1} are attributed to Si–O–Al and Si–O–Mg bonds. This indicated that most part of the layer charge resulted from trivalent (Al^{3+}, Fe^{3+}) to bivalent (Mg^{2+}) ion substitution in the octahedral sheet. The 3446 cm^{-1} and 1645 cm^{-1} bands corresponded to OH frequencies of the water molecule. Table 3 presents the bands related to OH groups of dioctahedral smectites and the corresponding assignment of the bentonite fraction, according to Farmer (1974). The band around 2350 cm^{-1} was from the room CO_2.

3.1.4. Thermoanalysis

Fig. 5 and Table 4 show the TG analyses and Fig. 6 the DTA data corresponding to the bentonite fraction. The mass losses observed in the range from room temperatures (RT) to 200 °C are related to the removal of adsorbed and interlayer water molecules. From 400 °C to

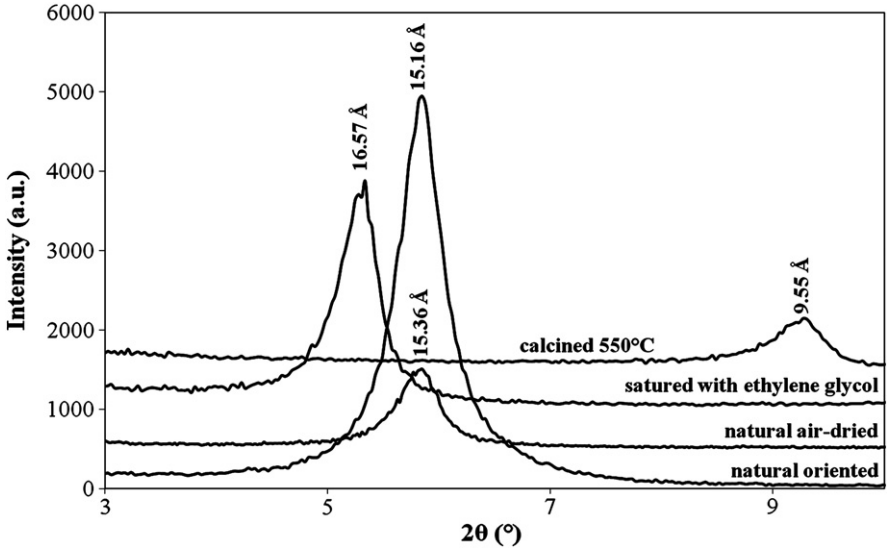

Fig. 2. X-ray pattern of air-dried bentonite (AD) of bentonite and after saturation with ethylene glycol (EG) and calcination.

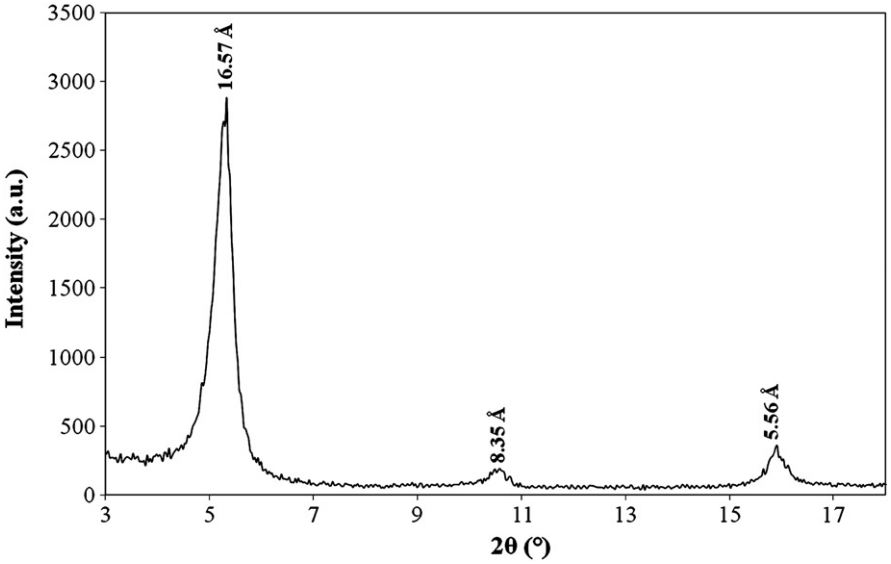

Fig. 3. X-ray pattern of the ethylene glycol solvated sample (EG).

Table 2
Chemical composition of the bulk bentonite (in mass %).

SiO_2	Al_2O_3	Fe_2O_3	MnO	MgO	CaO	Na_2O	K_2O	TiO_2	P_2O_5	LOI	Total
59.69	21.23	1.71	0.14	5.89	3.02	Nd	0.29	0.31	0.02	7.66	99.96

Nd: not detected.
LOI: loss on ignition at 1000 °C.

800 °C the mass losses are due to dehydroxylation (Ayaria et al., 2005; Yurdakoc et al., 2008).

3.2. Influence of high pressure

3.2.1. XRD pattern of bentonite after high pressure application

There was no difference between the patterns of the pristine sample and the processed sample (Fig. 7).

After the HP experiments, the samples were placed inside a container with controlled humidity and the XRD analysis was performed few hours after the experiments. Therefore, data suggested that there was no change of the interlayer water content after the experiment and if any structural change up to 7.7 GPa has occurred it was reversible when pressure was removed.

Table 3
Relation between the FTIR bands and the OH-groups for dioctahedral smectites (after Farmer, 1974).

OH bending vibration zone (cm^{-1})	OH stretching vibration zone (cm^{-1})	OH group
916	3621	Al–Al–OH
848	3670	Al–OH–Mg
788		Fe^{3+}–OH–Mg
670		Si–O–Mg
628		Si–O–Al
1030		Si–O
466 and 522		Low frequency SiO
1114		High frequency SiO
1645	3446	H_2O

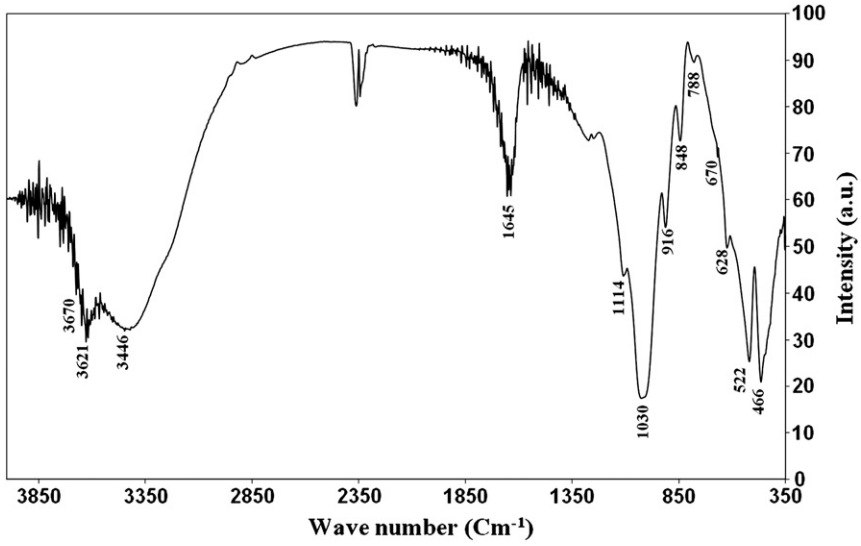

Fig. 4. FTIR spectra of bentonite fraction (KBr pellets with 1% bentonite).

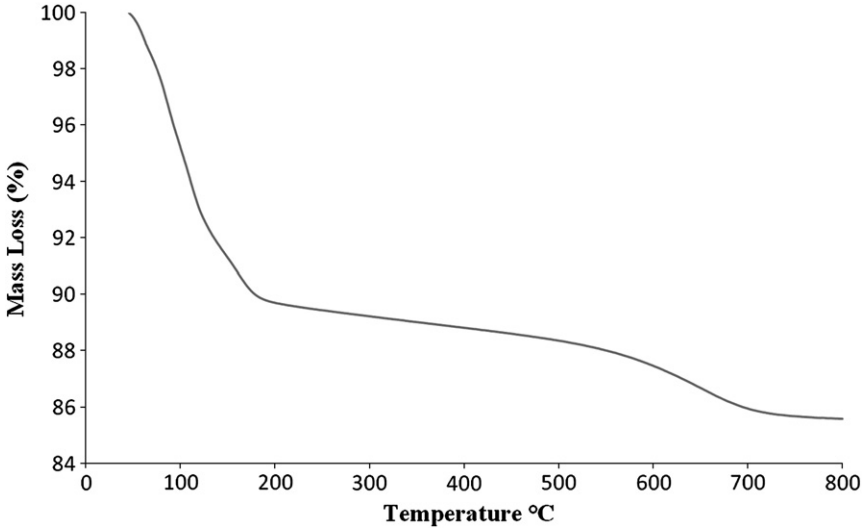

Fig. 5. TGA curve of the bentonite fraction.

Table 4
Thermogravimetric mass loss of the bentonite fraction.

Temperature range	Mass loss (%)
RT–200 °C	8.7
200–500 °C	1.4
500–800 °C	2.8
RT–800 °C	12.9

3.2.2. In-situ FTIR measurements of bentonite in the DAC up to 8 GPa

Fig. 8 shows the results obtained from in-situ FTIR measurements of bentonite in the DAC from ambient pressure up to 7.6 GPa. Only the 1030 cm^{-1} band, associated to the Si–O bond, shifted appreciably under pressure in a reversible way (Fig. 9), probably due to the pressure induced approximation of the tetrahedral sheet. After pressure release, the frequency of this band shifted back to the original value.

The pressure induced decrease of the basal spacing approximated the tetrahedral sheets. This behavior was reversible upon pressure release. The shift of the Si–O band could also be related to the intrinsic stress induced during the phase transformation of water into ice inside the interlayer spacing.

The band at ~1645 cm^{-1} is related to molecular H_2O and the band at 3000–3600 cm^{-1} is related to stretching modes of OH groups. These bands remained practically unchanged under high pressure (Fig. 8).

3.2.3. In-situ FTIR measurements of bentonite in the DAC up to 13 GPa

Fig. 10 shows the FTIR spectra of bentonite fraction not dispersed in KBr up to 13 GPa. The transmittance of the bands related to the smectite structure was practically zero for samples not dispersed in KBr (strong absorption). However, it was still possible to detect the bands related to H_2O and OH in the structure up to 13 GPa. The width of the band at ~1645 cm^{-1} increased while its intensity decreased at high pressures, probably due to the phase transformation of water into ice. The behavior of this band was reversible during pressure release and its position remained practically unchanged. A similar behavior was observed in the 3000–3600 cm^{-1} region related to OH, probably due to the OH frequencies of the water molecule (Fig. 10).

It is important to point out that the processing of pure montmorillonite in the DAC was certainly less hydrostatic than the processing of the sample dispersed in KBr, which is a soft solid material. Particularly at very high pressures, non-hydrostatic effects should affect the vibration modes.

As pressure increased at ambient temperature, liquid water transformed to tetragonal ice VI at ~1 GPa, and to cubic ice VII at ~2 GPa (Lin et al., 2004; Somayazulu et al., 2008). The phase transition of the interlamellar water into ice (VI or VII) hindered the desorption of water due to the smaller diffusion coefficient of the solid phase. The

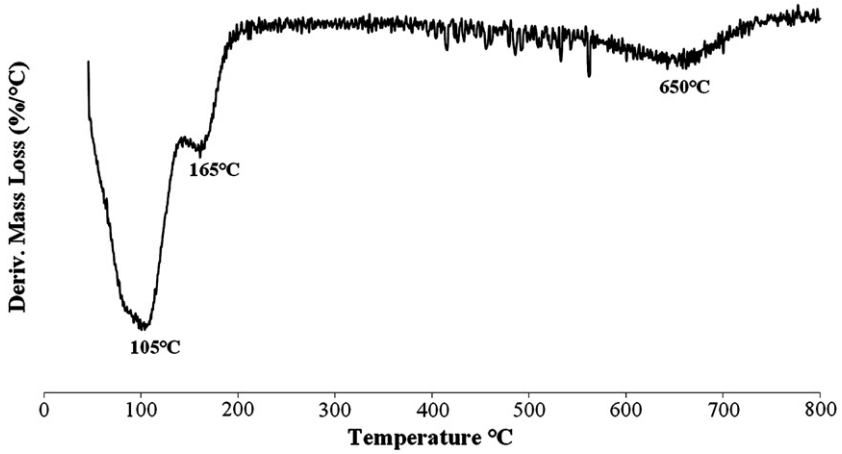

Fig. 6. DTA curve of the bentonite fraction.

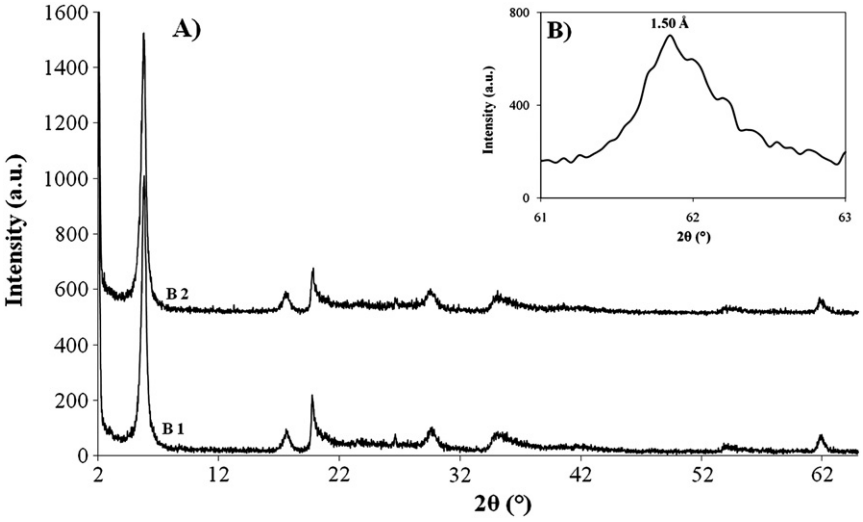

Fig. 7. A) XRD patterns of the bentonite before (B1) and after (B2) 7.7 GPa at RT during 30 min. B) 060 reflection of sample B2.

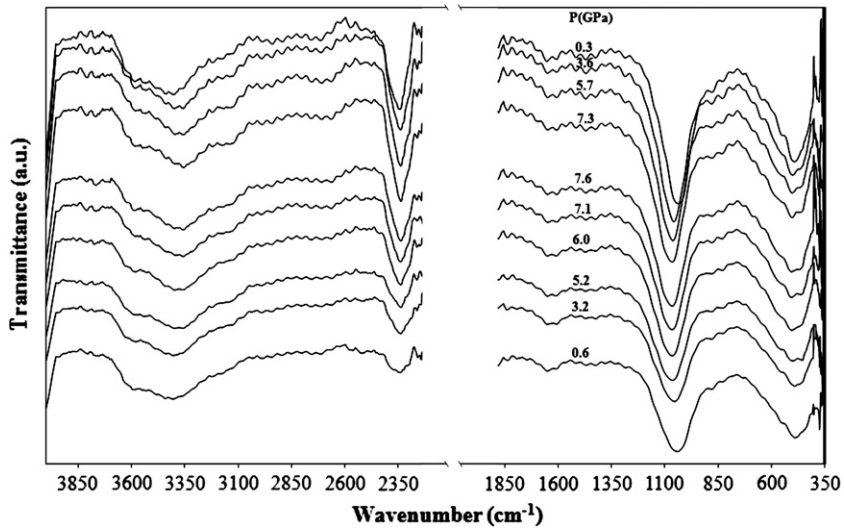

Fig. 8. FTIR spectra of the bentonite (1% m/m of bentonite in KBr) up to 7.6 GPa and during the pressure release.

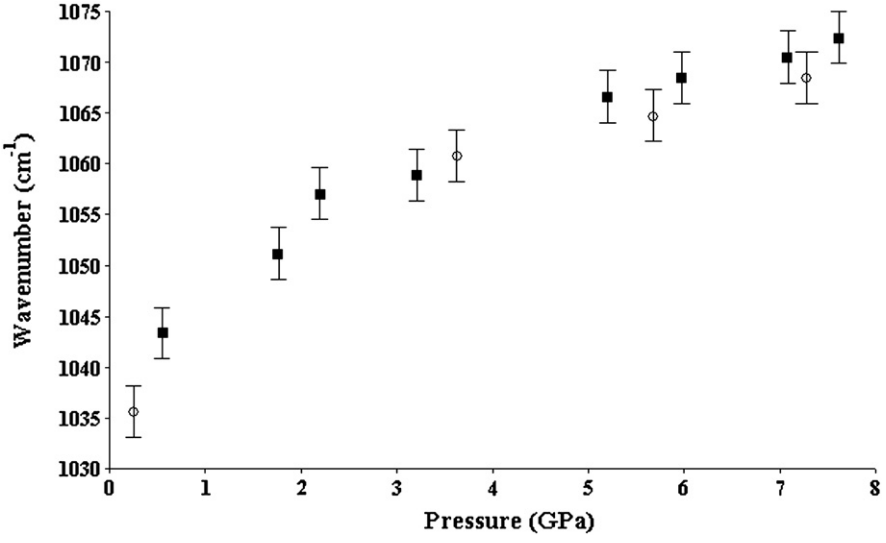

Fig. 9. Pressure dependence of the Si–O band from ambient pressure up to 7.6 GPa (■) and during pressure release (○).

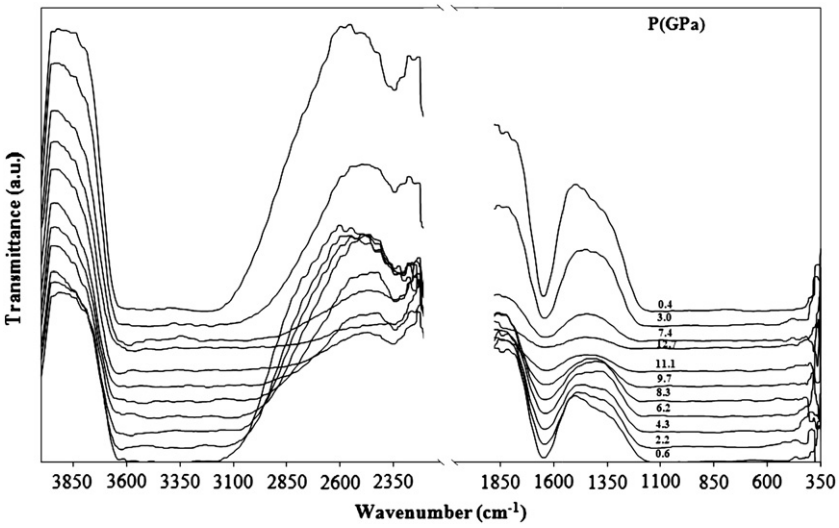

Fig. 10. FTIR spectra of bentonite up to 13 GPa.

higher the pressure, the higher the temperature necessary to desorb the water from the interlayer spaces (Koster van Groos and Guggenheim, 1987), according to the temperature–pressure phase diagram of water.

4. Conclusions

The montmorillonite structure was stable under high pressure and did not present significant structural changes up to 8 GPa. The only change observed at high pressure was the shift of the Si–O band to higher wavenumbers. Under pressure, the layers approximate, affecting the vibration modes of the water and ice molecules in the interlayer spaces and also of the Si–O bands. This behavior was reversible.

Since clay minerals have been used as a barrier in radioactive waste disposal facilities to minimize the migration of contaminants, the present finding that montmorillonite structure remains stable and does not lose H_2O under high pressure due to the phase transition of the interlamellar water into ice (VI or VII), points to its ability to still act as a clay barrier under high pressure conditions.

Acknowledgments

We would like to thank Dr. Marcia Gallas for all the research guidance given during the experiments with toroidal chambers. This research was financially supported by the Brazilian Institutions CNPq, CAPES and CNEN.

References

Alabarse, F. G., 2009. Análise da estabilidade estrutural da esmectita sob altas pressões e altas temperaturas. Master Thesis, UFRGS, Porto Alegre, Brasil

Ayaria, F., Srasrab, E., Trabelsi-Ayadia, M., 2005. Characterization of bentonitic clays and their use as adsorbent. Desalination 185, 391–397.

Bergaya, F., Theng, B.K.G., Lagaly, G., 2006. Handbook of clay science. Developments in Clay Science, Volume 1. Elsevier Science, Amsterdam.

Borchardt, G.A., 1977. Montmorillonite and other smectite minerals. In: Dixon, J.B., Weed, S.B. (Eds.), Minerals in Soil Environments. Soil Science Society of America, Madison, Wisconsin, pp. 299–330.

Brunauer, S., Emmett, P.H., Teller, E., 1938. Adsorption of gases in multimolecular layers. Journal American Chemical Society 60, 309–319.

Calarge, L. M., 2001. Estudo mineralógico e geoquímico de bentonitas do sul da Bacia do Paraná (Aceguá, Brasil e Melo Uruguai). Ph.D. thesis, UFRGS, Porto Alegre, Brasil

Calarge, L., Meunier, A., Formoso, M.L., 2003. A bentonite bed in the Aceguá (RS, Brazil) and Melo (Uruguay) areas: a highly crystallized montmorillonite. Journal of South American Earth Sciences 16, 187–198.

Caillére, S., Hénin, S., Rautureau, M., 1982. Minéralogie des Argiles. 1: structure et propriétés physico-chimiques. Masson, Paris, pp. 70–80.

Farmer, V.C., 1974. The layers silicates: the infrared spectra of minerals. Mineralogical Society, London 331–363.

Greene-Kelly, R., 1953. The identification of montmorillonoids in clays. Journal of soil science 4, 233–237.

International Atomic Energy Agency, 2006. Geological Disposal of Radioactive Waste, Safety Requirements No WS-R-4, Vienna.

Koster van Groos, A.F., Guggenheim, S., 1987. Dehydration of a Ca- and a Mg-exchanged montmorillonite (Swy-1) at elevated pressures. Am. Mineral 72, 292–298.

Khvostantsev, L. G., 1984. High temperatures–high pressures, 16, 165.

Lin, J., Militzer, B., Struzhkin, V.V., Gregoryanz, E., Hemley, R.J., Mao, H., 2004. High pressure–temperature Raman measurements of H_2O melting to 22 GPa and 900 K. The Journal of chemical physics (ISSN: 0021-9606) vol. 121 (17), 8423–8427 CODEN JCPSA6.

Madejová, J., Janek, M., Komadel, P., Herbert, H.-J., Moog, H.C., 2002. FTIR analyses of water in MX-80 bentonite compacted from high salinary salt solution systems. Applied Clay Science 20, 255–271.

Nakazawa, H., Yamada, H., Fujita, T., 1992. Crystal synthesis of smectite applying very high pressure and temperature. Applied Clay Science vol. 6 (5–6), 395–401.

Piermarini, G.J., Block, S., 1975. Rev. Sci. Instrum. 46, 973.

Piermarini, G.J., Block, S., Barnett, J.D., Forman, R.A., 1975. Journal of Applied Physics 46, 2774–2780.

Pusch, R., 2006. Clays and nuclear waste management. In: Bergaya, F., Theng, B.K.G., Legaly, G. (Eds.), Handbook of Clay Science. : Developments in Clay Science, volume 1. Elsevier, Amsterdam, pp. 703–716.

Rosenquist, I.Th., 1959. Montmorillonitt fra Skyverdalen i Hemseedal. Norsk Geologisk Tidsskrift 39, 350.

Sherman, W.F., Stadtmuller, A.A., 1987. Experimental Techniques in High-pressure Research. John Wiley & Sons Ltd., London.

Somayazulu, M., Shu, J., Zha, C., Goncharov, A., 2008. In situ high-pressure X-ray diffraction study of H_2O ice VII. The Journal of Chemical Physics 128, 064510.

Van Geet, M., Volckaert, G., Bastiaens, W., Maes, N., Weetjens, E., Sillen, X., Vallejan, B., Gens, A., 2007. Efficiency of a borehole seal by means of pre-compacted bentonite blocks. Physics and Chemistry of the Earth 32, 123–134.

Yurdakoç, M., Akçay, M., Tonbul, Y., Ok, F., Yurdakoç, K., 2008. Preparation and characterization of Cr- and Fe-pillared bentonites by using $CrCl_3$, $FeCl_3$, $Cr(acac)_3$ and $Fe(acac)_3$ as precursors. Microporous and mesoporous materials (ISSN: 1387-1811) vol. 111 (1–3), 211–218.